Am J Physiol Endocrinol Metab 304: E1188–E1198, 2013.
First published March 26, 2013; doi:10.1152/ajpendo.00560.2012.

Expression of SHP-1 induced by hyperglycemia prevents insulin actions in podocytes

Nicolas Drapeau,[1]* Farah Lizotte,[1]* Benoit Denhez,[1] Andréanne Guay,[1] Chris R. Kennedy,[2] and Pedro Geraldes[1]

[1]*Clinical Research Center Étienne Le-Bel and Division of Endocrinology, Departments of Medicine, Université de Sherbrooke, Québec, Canada; and* [2]*Kidney Research Center, Ottawa Hospital Institute, Ottawa, Ontario, Canada*

Submitted 7 November 2012; accepted in final form 24 March 2013

Drapeau N, Lizotte F, Denhez B, Guay A, Kennedy CR, Geraldes P. Expression of SHP-1 induced by hyperglycemia prevents insulin actions in podocytes. *Am J Physiol Endocrinol Metab* 304: E1188–E1198, 2013. First published March 26, 2013; doi:10.1152/ajpendo.00560.2012.— Renal podocyte apoptosis is an early event of diabetic nephropathy progression. Insulin action is critical for podocyte survival. Previous studies demonstrated that Src homology-2 domain-containing phosphatase-1 (SHP-1) is elevated in renal cortex of type 1 diabetic mice; we hypothesized that hyperglycemia-induced SHP-1 expression may affect insulin actions in podocytes. Type 1 diabetic Akita mice ($Ins2^{+/C96Y}$) developed elevated foot process effacement and podocyte apoptosis compared with control littermate mice ($Ins2^{+/+}$). In contrast to $Ins2^{+/+}$ mice, insulin-stimulated protein kinase B (Akt) and extracellular signal-regulated kinase (ERK) phosphorylation were remarkably reduced in renal podocytes of Akita mice. This renal insulin resistance was associated with elevated SHP-1 expression in the glomeruli. Cultured podocytes exposed to high glucose concentration (HG; 25 mM) for 96 h exhibited high levels of apoptotic markers and caspase-3/7 enzymatic activity. HG exposure raised mRNA and protein levels of SHP-1 and reduced the insulin-signaling pathway in podocytes. Overexpression of dominant-negative SHP-1 in podocytes prevented HG effects and restored insulin actions. Elevated SHP-1 expression induced by high glucose levels was directly associated with insulin receptor-β in vitro and in vivo to prevent insulin-stimulated Akt and ERK phosphorylation. In conclusion, our results showed that high levels of SHP-1 expression in glomeruli cause insulin resistance and podocyte loss, thereby contributing to diabetic nephropathy.

insulin signaling; protein tyrosine phosphatase; insulin receptor-β; Src homology-2 domain-containing phosphatase-1

DIABETIC NEPHROPATHY (DN) is the leading cause of end-stage renal disease worldwide and an independent risk factor for all-cause and cardiovascular mortalities in diabetic patients (5, 30). Podocytes and their foot processes are unique in that they comprise the outer layer of the kidney ultrafiltration barrier and form the glomerular slit diaphragm, which is a complex cellular structure that prevents the development of proteinuria in an actin cytoskeleton-dependent manner (37). Careful morphometric examination of renal biopsies in subjects with type 1 and type 2 DM revealed that the density of podocytes is significantly reduced in patients with short duration of diabetes before the onset of microalbuminuria and more advanced DN (21, 28, 39). Among various morphological characteristics, a decreased number of podocytes in the glomeruli is the strongest predictor of DN progression (21).

Several studies provide support for an "insulin resistance"-renal link in type 1 diabetes (12). Yip and colleagues have reported that 14 type 1 diabetic subjects with microalbuminuria had significantly lower glucose disposal during euglycemic-hyperinsulinemic clamp studies than did matched controls, even after accounting for blood pressure and body mass index (40). Previous reports have correlated insulin-signaling pathways with podocyte function and survival (18, 21). Coward and colleagues showed that podocytes are insulin-responsive cells. Insulin induced an acute increase in glucose uptake in cultured podocyte cell lines and in human podocytes ex vivo due to translocation of the glucose transporters GLUT-1 and GLUT-4 to the plasma membrane (6, 23). Interestingly, renal disease similar to DN can be observed in patients with a genetic mutation of the insulin receptor (IR) (25). More recently, Welsh and colleagues engineered mouse models in which the gene encoding the IR was deleted in a podocyte-specific manner (38). In these animals, albuminuria developed, along with effacement of the podocyte foot processes, apoptosis, thickening of the glomerular basement membrane, and increased glomerulosclerosis, all histological features typical of DN. However, much less studied is how toxic metabolites of glucose result in abnormal insulin actions in podocytes.

We reported that the Src homology-2 domain-containing phosphatase-1 (SHP-1), a protein tyrosine phosphatase (PTP) that is critical in abating cell response to growth factors, is elevated in the retina and renal cortex by diabetes (11). SHP-1 has been shown to inhibit vascular endothelial growth factor (VEGF) actions in podocytes and renal glomeruli of diabetic rats and mice (22). Because SHP-1 is also known to interact with insulin actions (7), we hypothesized that hyperglycemia-induced SHP-1 expression may affect insulin signaling in podocytes and be responsible for insulin unresponsiveness in diabetic renal glomeruli leading to DN.

EXPERIMENTAL PROCEDURES

Reagents and antibodies. Fetal bovine serum (FBS), RPMI-1640, phosphate-buffered saline (PBS), and penicillin-streptomycin were obtained from Invitrogen. Primary antibodies for immunoblotting were obtained from commercial sources, including actin (horseradish peroxidase; I-19), SHP-1 (C-19), IR-β (29B4), insulin receptor substrate (IRS)-1 (C-20), phosphatase and tensin homolog (PTEN, C-20-R), and PTP1B (C-19) from Santa Cruz Biotechnology; IRS-2 (L1326), protein kinase B (Akt), extracellular signal-regulated kinase (ERK), phospho-Akt (D9E), and phospho-ERK (D13.14.4E) from Cell Signaling; monoclonal antibody against SHP-1 (NL213) and IRS-1 (AW58) from Millipore; purified monoclonal antibody against PTP1B (610139) and SHP-2 (610621) from BD Biosciences; monoclonal

* N. Drapeau and F. Lizotte contributed equally to this work.
Address for reprint requests and other correspondence: P. Geraldes, Université de Sherbrooke, 3001 12e Ave Nord, Sherbrooke, Québec, Canada J1H 5N4 (e-mail: Pedro.Geraldes@USherbrooke.ca).

Table 1. *Sequences of primers*

Gene	Forward	Reverse
mVEGF	GGAGTACCCCGACGAGATAGAGTA	AGCCTGCACAGCGCATC
mSHP-1	ATCAATGCCAACTACGTGAAGAAC	GGCTGGCGATGTAGGTCTTAGA
mSHP-2	CCTCAACACAACTCGTATCAATGC	TGTTGCTGGAGCGTCTCAAA
mPTP1B	CGGGAGGTCAGGGACCTT	GGGTCTTTCCTCTTGTCCATCA
mIR	CATGTGCAGGAATGGCTTGTT	TTCTGCGTTTTCTGCAGTGCTA
mIRS1	AATCCTCAGGAGTTCATTGACTGAA	TTCCGGTGTCACAGTGCTTTC
mIRS2	AGCAAGAACCTGACTGGTGTATACC	TCGCAATTGAGCTTCACGAA
mFN	CTTTGGCAGTGGTCATTTCAG	ATTCTCCCTTTCCATTCCCG
mCol IV	GGCGGTGCACAGTCAGACCAT	GGAATAGCCAATCCACAGTGA
mTGF-β	GGACACACAGTACAGCAA	GACCCACGTAGTAGACGAT
mGAPDH	GCATGGCCTTCCGTGTTC	GATGTCATCATACTTGGCAGGTTT

m, Mouse; VEGF, vascular endothelial growth factor; SHP-1, Src homology-2 domain-containing phosphatase-1; PTP, protein tyrosine phosphatase; IR, insulin receptor; IRS, insulin receptor substrate; FN, fibronectin; Col IV, collagen type IV; TGF, transforming growth factor.

antibody against IR-β (AB69508) from Abcam; isolectin B4-fluorescein isothiocyanate (FITC) conjugated from Vector Laboratories; and rabbit and mouse peroxidase-conjugated secondary antibody from Santa Cruz Biotechnology. All other reagents employed, including bovine serum albumin (fraction V), EDTA, leupeptin, phenylmethylsulfonyl fluoride, aprotinin, insulin, D-glucose, D-mannitol, and Na_3VO_4, were purchased from Sigma-Aldrich, unless otherwise stated.

Animal and experimental design. C57BL/6J and diabetic heterozygous male *Ins2*$^{+/C96Y}$ (Akita) mice were purchased from The Jackson Laboratory and bred in our animal facility. Throughout the period of study, animals were provided with free access to water and standard rodent chow (Harlan Teklad, Madison, WI). All experiments were conducted in accordance with the Canadian Council of Animal Care and Institutional Guidelines and were approved by the Animal Care and Use Committees of the University of Sherbrooke, according to National Institutes of Health (NIH) guidelines.

Blood glucose, urinary albumin excretion, and glomerular filtration rate measurements. Blood glucose was measured by a Glucometer (Contour; Bayer). Twenty-four-hour urine collections were obtained from mice 1 day before death by housing them in individual mouse metabolic cages (Nalgene, model 650-0311; Nalgene Nunc International, Rochester, NY) with free access to water and rodent mash. Urinary creatinine concentration was measured using alkaline picrate colorimetry based on Jaffe reaction (The Creatinine Companion; Exocell, Philadelphia, PA), and albumin levels were measured using an indirect competitive enzyme-linked immunosorbent assay (ELISA) according to the manufacturer's instructions (Albuwell M; Exocell). The glomerular filtration rate (GFR) was evaluated using FITC-inulin clearance as described previously (29). Briefly, 5% FITC-inulin (3.74 μl/g of body wt) was injected retroorbitally, followed by collection of ~20 μl of saphenous vein blood at 3, 7, 10, 15, 35, 55, and 75 min post-FITC-inulin injection in conscious mice. Fluorescence was determined using Infinite 200 PRO NanoQuant (Tecan Group).

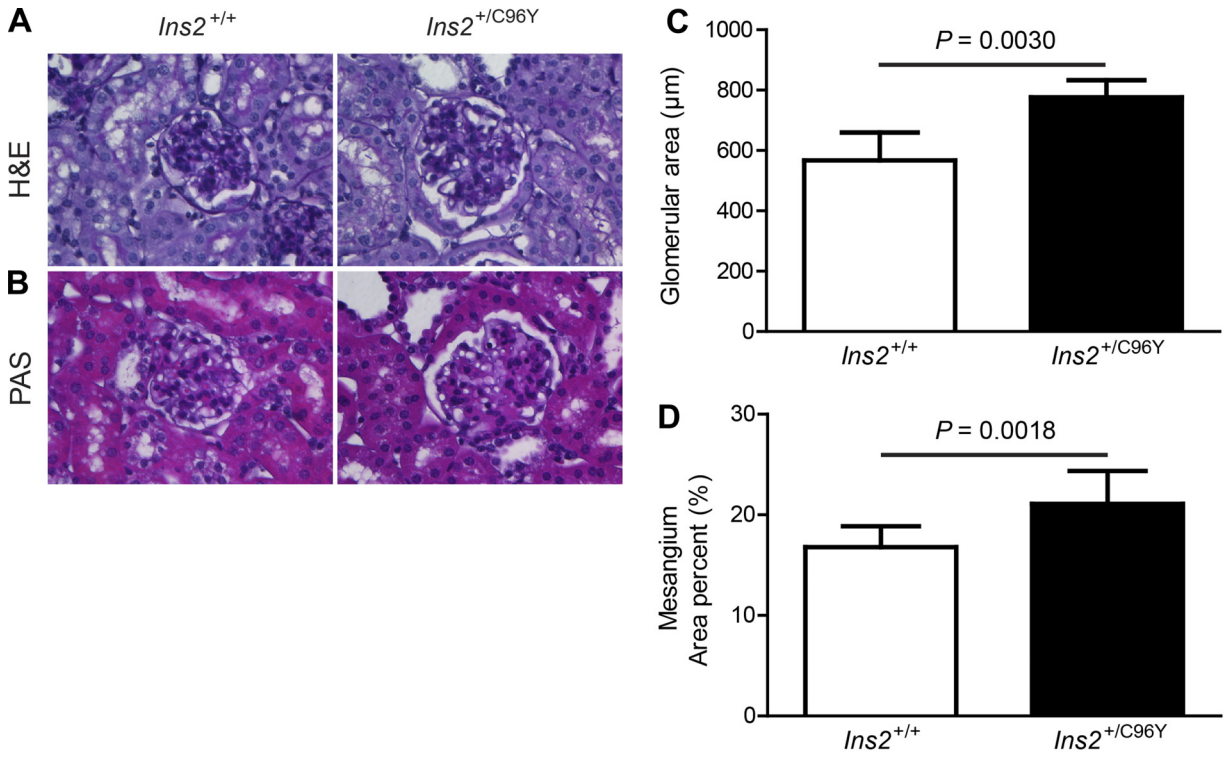

Fig. 1. Glomerular histopathology in type 1 diabetic Akita mice (*Ins2*$^{+/C96Y}$) mice. Six months of age renal glomeruli of control littermate mice (*Ins2*$^{+/+}$) and *Ins2*$^{+/C96Y}$ mice stained with hematoxylin and eosin (H&E, *A*) or periodic acid-Schiff (PAS, *B*). Quantification of glomerular hypertrophy (*C*) and mesangium expansion (*D*). Results are shown as means ± SD of 3–4 glomeruli of 11 mice/group.

Histopathology and transmission electron microscopy. Left mouse kidneys were harvested for pathological examination, and sections were fixed in 4% paraformaldehyde (Sigma-Aldrich, St. Louis, MO) for 24 h and then transferred to 90% ethanol for immunohistochemistry. The tissue was embedded in paraffin, and 6-μm sections were stained with periodic acid-Schiff stain and hematoxylin and eosin (Sigma). Right mouse kidneys were used for transmission electron microscopy to evaluate podocyte structure and foot process effacement. Fifteen glomerular tufts per animal were chosen randomly for analysis. To assess for foot process effacement, the mean width of foot processes was evaluated in electron micrographs of both groups. Effacement is defined as >2.5-fold increase in mean width. Microscope analyses were performed in a blinded fashion.

Mesangium expansion, glomerular hypertrophy, and quantitation of podocyte apoptosis. Mesangial matrix expansion was evaluated quantitatively by measuring the relative number of pixels of the mesangium divided by the total area of each glomerulus, by adjusting the threshold permitting a binary analysis using Image J (NIH, Bethesda, MD). Apoptotic nuclei of kidney sections were detected using the TACS 2 Tdt-Fluor in situ apoptosis detection kit (Trevigen, Gaithersburg, MD) according to the manufacturer's instructions. Podocytes were stained using antibody against nephrin followed by incubation with secondary antibody Alexa-594-conjugated anti-goat (1:500; Jackson ImmunoResearch Laboratories). Apoptotic podocytes were counted when both podocyte markers and Tdt-fluorescein-positive cells colocalized on all glomeruli (20–30) on the transverse section of the left kidney.

Immunofluorescence. Kidneys from *Ins2*$^{+/+}$ and *Ins2*$^{+/C96Y}$ mice were frozen in optimum-cutting temperature (OCT) compound (BDH) embedding resin in cryomolds on a block of dry ice and sectioned at 8 μm (Leica Cryostat). The sections were fixed with cold methanol, blocked in PBS containing 10% goat serum for 1 h, exposed in sequence to primary antibodies (nephrin, phospho-Akt, 1:100) overnight following by incubation with secondary antibodies Alexa-647-conjugated anti-rabbit IgG (1:500; Jackson ImmunoResearch Laboratories) and 7-amino-4-methylcoumarin-3-acetic acid-conjugated anti-goat IgG (1:500; Abcam) in mounting media (Vectashield; Vector Laboratories, Burlingame, CA). Images were taken using a Zeiss laser scan microscope equipped with a ×63 water immersion objective or a Zeiss fluorescence microscope equipped with ×10 and ×40 objectives; images of one experiment were taken at the same time under identical settings and handled in Adobe Photoshop similarly across all images.

Laser capture microdissection. Animals were killed, and kidney was removed and immediately whole mounted in OCT. Eight-micrometer-thick renal cryosections were cut, thaw mounted on nonadhesive glass slides, and then placed immediately on dry ice following fixation for 30 s in 75% ethanol and then dehydration through a series of alcohol gradients, and cleared for 4 min in xylene (Fluka). Sections were air-dried in a fume hood for 2 min and then subjected to laser microdissection using the PixCell laser capture microscope (Arcturus Engineering, ABI). Sections were also stained with isolectin-B4-FITC. Multiple glomeruli were harvested from the sections for VEGF, SHP-1, and transforming growth factor (TGF)-β mRNA expression.

Cell culture. The mouse podocyte cell line (32) was used and cultured as previously described (24). In brief, cells were grown under permissive conditions at 33°C in RPMI-1640 media containing 10% FBS, 50 U/ml interferon-γ (IFNγ), and 100 U/ml of penicillin/streptomycin in collagen-coated flasks. The IFNγ concentration was gradually reduced to 10 U/ml in successive passages. Next, cells were trypsinized and subcultured without IFNγ and were allowed to differentiate at 37°C for 14 days with media changes on alternate days. After differentiation of podocytes, medium was changed to RPMI 0.1% FBS containing normal glucose (NG; 5.6 mM + 19.4 mM

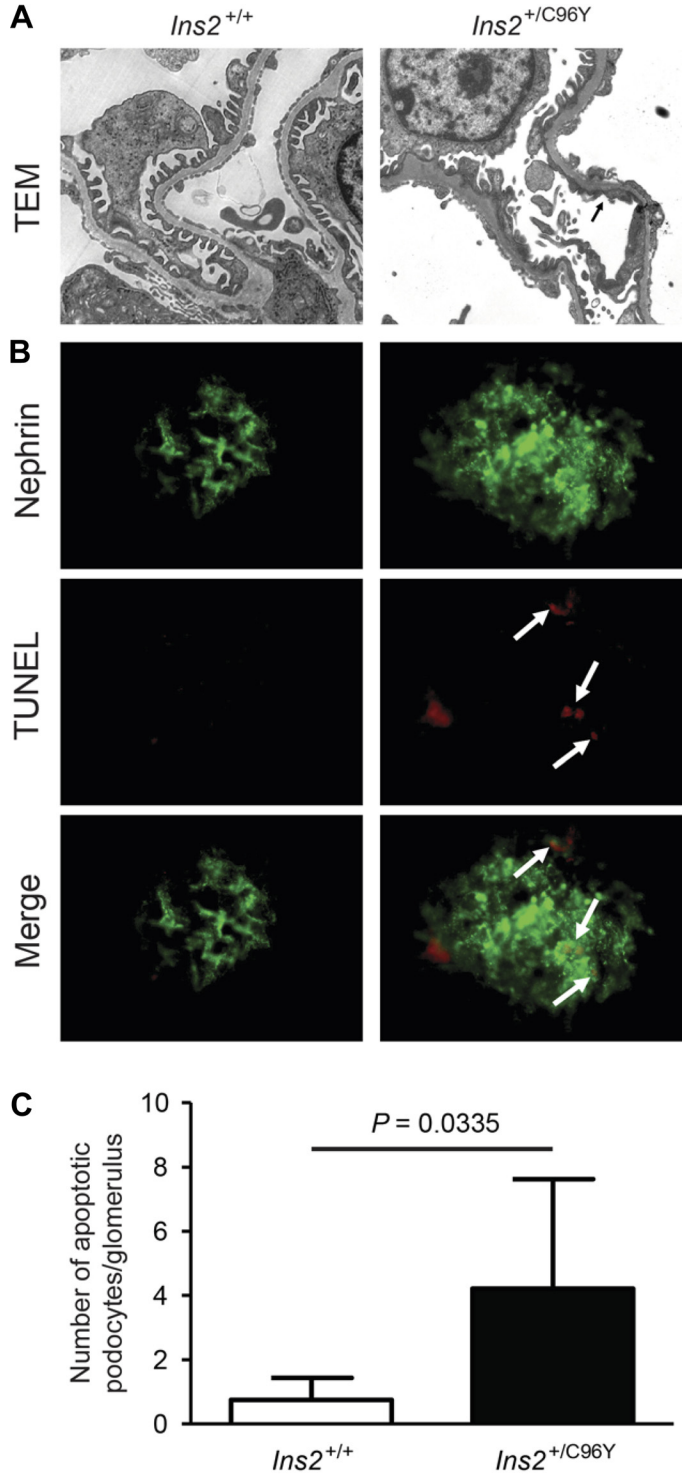

Fig. 2. Foot process effacement and podocyte apoptosis. *A*: transmission electronic microscopy (TEM) of podocyte foot process effacement (arrow). *B* and *C*: brightfield and immunofluorescence microscopy (*B*) and quantification of apoptotic-positive cells (red; arrows) and podocyte (nephrin; green) (*C*) in the glomerulus of *Ins2*$^{+/+}$ and *Ins2*$^{+/C96Y}$ mice. TUNEL, TdT-dUTP nick end-labeling. Results are shown as means ± SD of 3–4 glomeruli of 11 mice/group.

mannitol to adjust osmotic pressure) or high glucose (HG; 25 mM) up to 96 h.

Adenoviral vector transfection. Adenoviral vectors containing green fluorescent protein (GFP, Ad-GFP), and dominant-negative (Ad-dnSHP-1) or wild-type (Ad-wtSHP-1) SHP-1 and were generously gifted by Dr. A. Marette (Laval University) as previously described (7) and used to infect podocytes as we have reported previously in vascular cells (11, 14). Cultured mouse podocytes were infected with described adenoviral vectors at a multiplicity of infection of 75 in serum-free media for 2 h in a 37°C incubator supplemented with 5% CO_2, and adenovirus with the same parental genome carrying Ad-GFP gene was used as control. The cells were then grown in media containing 10% FBS for an additional 24 h in the incubator. Media of infected cells were removed and replaced by RPMI 0.1% FBS with additional 20 mM glucose for 96 h. Infectivity of these adenoviruses was evaluated by the percentage of green light-emitting cells under a fluorescent microscope (Nikon, Avon, MA). The presence of ~80% of Ad-GFP-positive cells was considered to be a successful infection and used for further experimentation.

DNA fragmentation analyses. DNA fragmentation was measured by quantitation of cytosolic oligonucleosome-bound DNA using ELISA (Roche Molecular Biochemicals) according to the manufacturer's instructions. Briefly, cells were grown in six-well plates at a density of 5×10^4 cells/well in 2 ml RPMI and 10% FBS. Podocytes were exposed to HG (96 h) in the presence or absence insulin (10 nmol/l) and then lysed directly on the plate.

Coimmunoprecipitation and immunoblot analyses. Cells were stimulated with the conditions and compounds indicated after overnight starvation. Renal cortex and cells were lysed in immunoprecipitation buffer [50 mM Tris (pH 6.8) and 10% glycerol] or Laemmli buffer [50 mM Tris (pH 6.8), 2% SDS, and 10% glycerol] containing protease inhibitors (1 mmol/l phenylmethylsulfonyl fluoride, 2 μg/ml aprotinin, 10 μg/ml leupeptin, and 1 mmol/l Na_3VO_4; Sigma). Protein amount was measured with a BCA kit (Bio-Rad). The lysates (500 μg of protein) were incubated with 1 μg specific antibody against SHP-1, IRS-1, or IR-β. Next, 50 μl protein A/G agarose beads (Santa Cruz Biotechnology) were added to the mix and rotated at 4°C for 90 min. Proteins linked to beads were pelleted and mixed with 25 μl of 2× Laemmli buffer. For immunoblot, 5–100 μg of protein were separated by SDS-PAGE, transferred to a polyvinylidene difluoride membrane, and blocked with 5% skim milk. Antigens were detected using anti-rabbit horseradish peroxidase-conjugated antibody for other Western blotting and detected with the enhanced chemiluminescence system (Pierce Thermo Fisher, Piscataway, NJ). Protein content quantification was performed using computer-assisted densitometry (Image J; NIH).

Real-time PCR analyses. Real-time PCR was performed to evaluate mRNA expressions of VEGF, SHP-1, IRS-1, IRS-2, IR-β, collagen type IV, TGF-β, and fibronectin. Total RNA was extracted from renal cortex or cultured podocytes with TRI-REAGENT, as described by the manufacturer, and an RNeasy mini kit (Qiagen, Valencia, CA). The RNA was treated with deoxyribonuclease I (Invitrogen) to re-

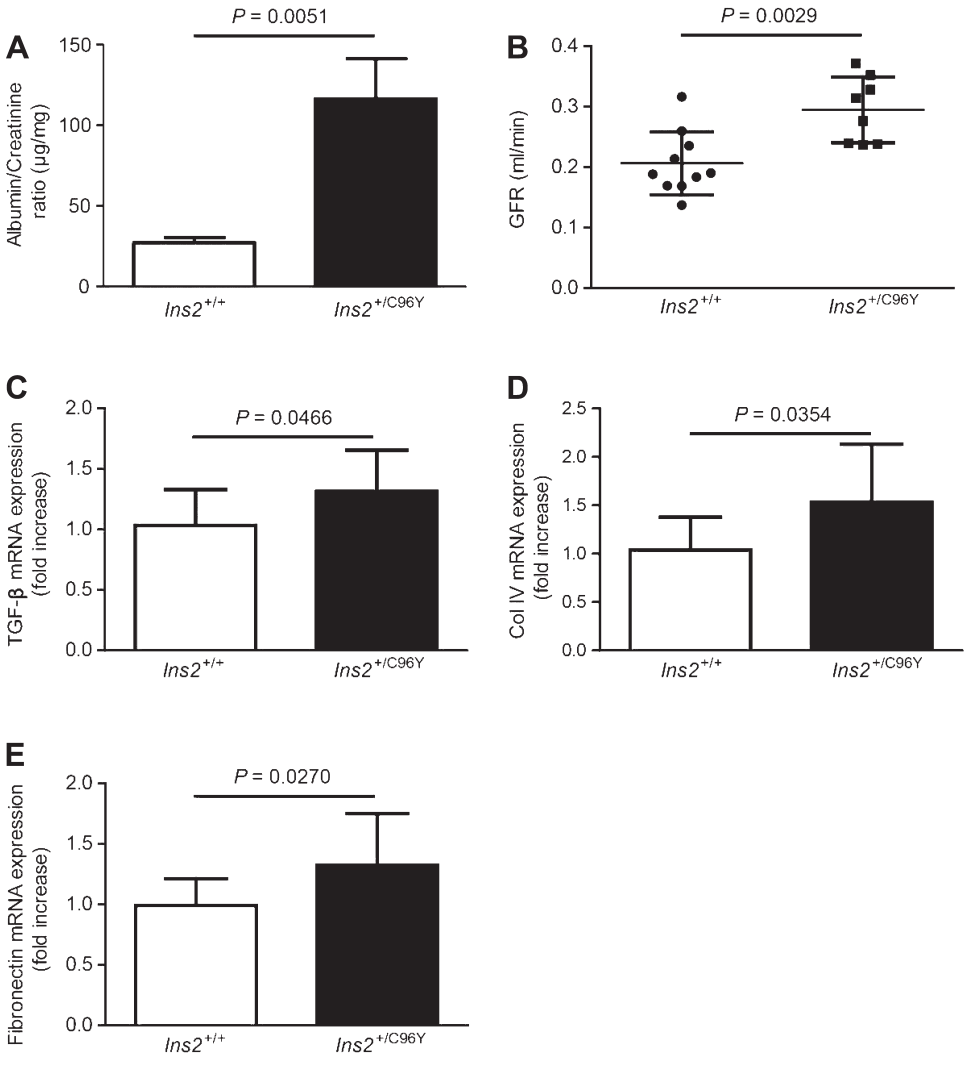

Fig. 3. Renal function and marker expression of diabetic nephropathy. Urine albumin creatinine ratio (*A*), glomerular filtration rate (GFR, *B*), and mRNA expression of transforming growth factor (TGF)-β (*C*), collagen type IV (Col IV, *D*), and fibronectin (*E*) in renal cortex of $Ins2^{+/+}$ and $Ins2^{+/C96Y}$ mice. Results are shown as means ± SD of 3–4 glomeruli of 11 mice/group. Results are shown as means ± SD of 6–10 mice/group.

move any genomic DNA contamination. Approximately 1 μg RNA was used to generate cDNA using SuperScript III reverse transcriptase and random hexamers (Invitrogen) at 50°C for 60 min. PCR primers are listed in Table 1. GAPDH mRNA expression was used for normalization. PCR products were gel purified, subcloned using a QIA quick PCR Purification kit (Qiagen), and sequenced in both directions to confirm identity.

Caspase-3/7 assay. Caspase-3 and -7 enzymatic activity was determined by quantification of cleaved substrate using luminescent assay Caspase 3/7 Glo (Promega, Fitchburg, WI) according to the manufacturer's instructions. Cells were stimulated as indicated and then lysed in Laemmli buffer. The same volumes of protein extract and reagent were mixed in a black-walled 96-well plate, and luminescence was determined using Infinite M1000 PRO (Tecan Group).

Statistical analyses. The data were shown as means ± SD for each group. Statistical analysis was performed by unpaired *t*-test or by one-way ANOVA followed by Tukey's test correction for multiple comparisons. All results were considered statistically significant at $P < 0.05$.

RESULTS

Type 1 diabetic Akita mice ($Ins2^{+/C96Y}$) exhibited podocyte loss and renal pathology. Renal pathology (glomerular hypertrophy and mesangial cell expansion) and function (urine albumin-to-creatinine ratio and GFR) have been previously reported in diabetic $Ins2^{+/C96Y}$ compared with control littermates (14). As expected, glomerular hypertrophy was increased at 6 mo of age in $Ins2^{+/C96Y}$ mice compared with nondiabetic mice ($P = 0.0030$) (Fig. 1, *A* and *C*). Blinded assessment of the mesangial cell expansion demonstrated a significant increase of extracellular matrix deposition in $Ins2^{+/C96Y}$ mice compared with nondiabetic control littermates ($P = 0.0018$) (Fig. 1, *B* and *D*). Increased renal pathology correlated with podocyte effacement and apoptosis. Transmission electron microscopy showed the presence of podocyte effacement (Fig. 2*A*) and positive apoptotic signal (TdT-dUTP nick end-labeling) in podocytes of $Ins2^{+/C96Y}$ mice compared with nondiabetic $Ins2^{+/+}$ mice (Fig. 2*B*). Furthermore, we observed that $Ins2^{+/C96Y}$ mice exhibited an increase of urine albumin-to-creatinine ratio by 3.3-fold ($P = 0.0051$) and elevated GFR (0.206 vs. 0.295 ml/min, $P = 0.0029$) compared with nondiabetic $Ins2^{+/+}$ mice (Fig. 3, *A* and *B*), which confirmed previous observations (27). Quantitative PCR analysis demonstrated that $Ins2^{+/C96Y}$ mice have elevated TGF-β, collagen type IV, and fibronectin mRNA expression (Fig. 3, *C*, *D*, and *E*), well known markers of glomerular injury.

Renal insulin resistance in $Ins2^{+/C96Y}$ mice. We injected insulin (5 mU/g iv) in $Ins2^{+/+}$ and $Ins2^{+/C96Y}$ mice to evaluate its signaling actions in the kidney. The right kidney was removed before the insulin injection to serve as an internal control (nonstimulated). Fifteen minutes after the injection (iv), insulin markedly increased IR-β, Akt, and ERK phosphorylation compared with unstimulated kidney of $Ins2^{+/+}$ mice. By contrast, insulin-induced IR-β, Akt, and ERK phosphorylation was significantly blunted in renal cortex of $Ins2^{+/C96Y}$ mice (Fig. 4*A*). To demonstrate unequivocally insulin resistance in

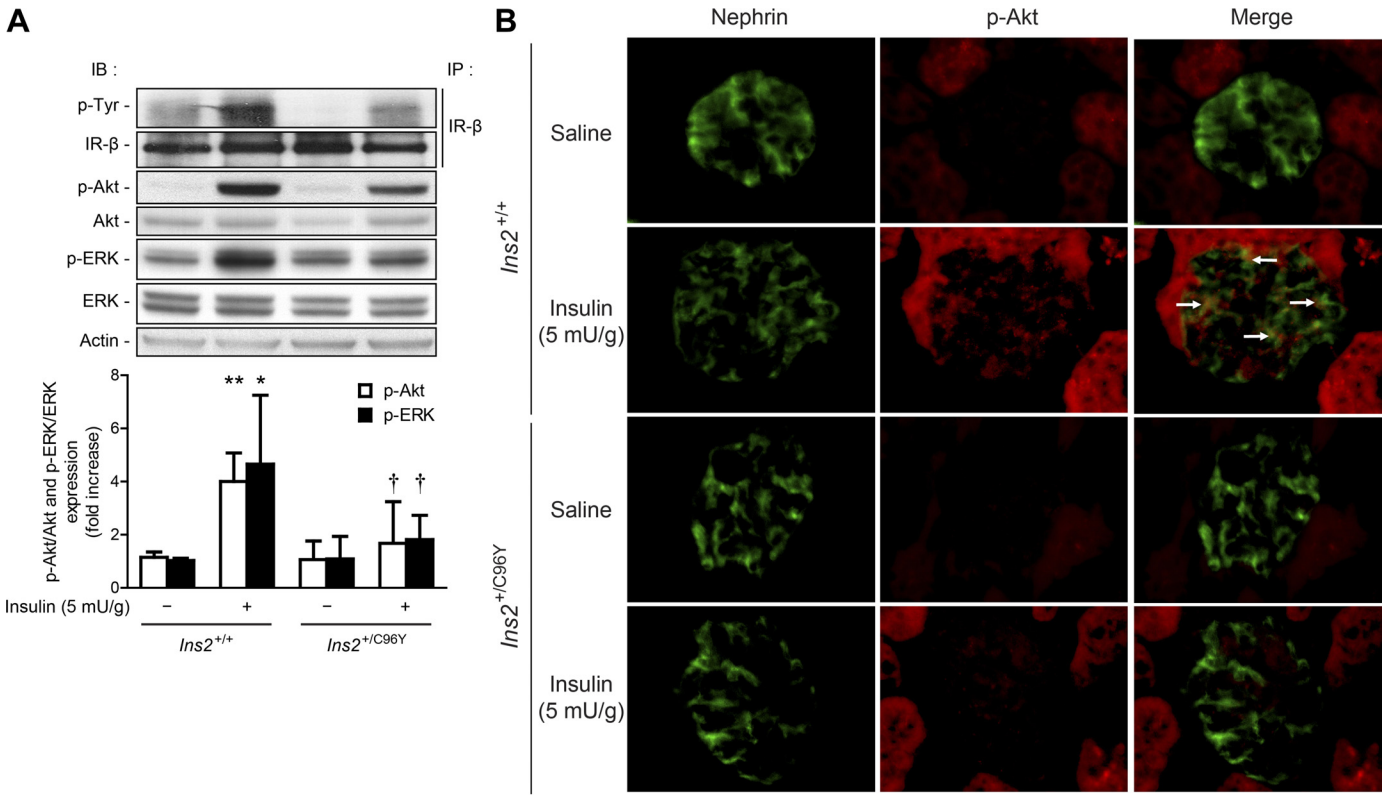

Fig. 4. Inhibition of insulin signaling in $Ins2^{+/C96Y}$ mice. Insulin injection (iv) for 15 min in 6 mo of age $Ins2^{+/+}$ and $Ins2^{+/C96Y}$ mice. *A*: expression of phosphor (p)-tyrosine [immunoprecipitated (IP) against insulin receptor (IR)-β], IR-β, phospho-protein kinase B (Akt), Akt, phospho-extracellular signal-regulated kinase (ERK), ERK, and actin was detected by Western blot, and densitometric quantitation was measured. *B*: immunofluorescence labeling of podocytes (nephrin; green) and phospho-Akt (red). Arrows represent colocalization of podocyte marker and phospho-Akt. Results are shown as means ± SD of 4–5 independent experiments. *$P < 0.05$ or **$P < 0.01$ vs. unstimulated $Ins2^{+/+}$ mice. †$P < 0.05$ vs. insulin-stimulated $Ins2^{+/+}$ mice.

podocytes of *Ins2*$^{+/C96Y}$ mice in vivo, immunofluorescence analysis of podocytes (nephrin) indicated that diabetic podocytes exhibited lower Akt phosphorylation compared with *Ins2*$^{+/+}$ mice after insulin stimulation (Fig. 4*B*). These findings suggest that hyperglycemia affects insulin signaling pathways in renal podocytes.

Increased SHP-1 expression modulates insulin unresponsiveness in diabetic glomeruli. We have previously reported that SHP-1 expression is elevated in renal cortex of streptozotocin-induced type 1 diabetic mice (11). We confirmed using a genetically modified type 1 diabetic model that SHP-1 mRNA and protein expression was elevated in renal cortex of *Ins2*$^{+/C96Y}$ mice (Fig. 5, *A* and *B*). Other protein phosphatases that have been previously shown to interact with the insulin-signaling pathway, such as PTEN, PTP1B, and SHP-2, were unchanged (Fig. 5, *A* and *B*). Furthermore, we confirmed by both immunofluorescence (Fig. 5*C*) and laser capture microdissection (Fig. 5*D*) that SHP-1 expression is definitely and significantly ($P = 0.0199$) elevated in the glomerular podocytes of *Ins2*$^{+/C96Y}$ mice, as well as other markers (VEGF and TGF-β) of glomerular injury (Fig. 5*D*).

Insulin inhibition and podocyte apoptosis in HG concentration. The effects of the high glucose condition on podocyte survival were measured by DNA fragmentation and caspase-3/7 enzymatic activity, markers of apoptosis. Exposing podocytes to HG levels for 96 h increased DNA fragmentation by 1.75-fold ($P = 0.0265$, Fig. 6*A*). The osmotic pressure was adjusted by adding a proper concentration of mannitol in the NG condition. Adding insulin (10 nmol/l) for 96 h partially reduced HG-induced podocyte apoptosis. However, insulin treatment for the

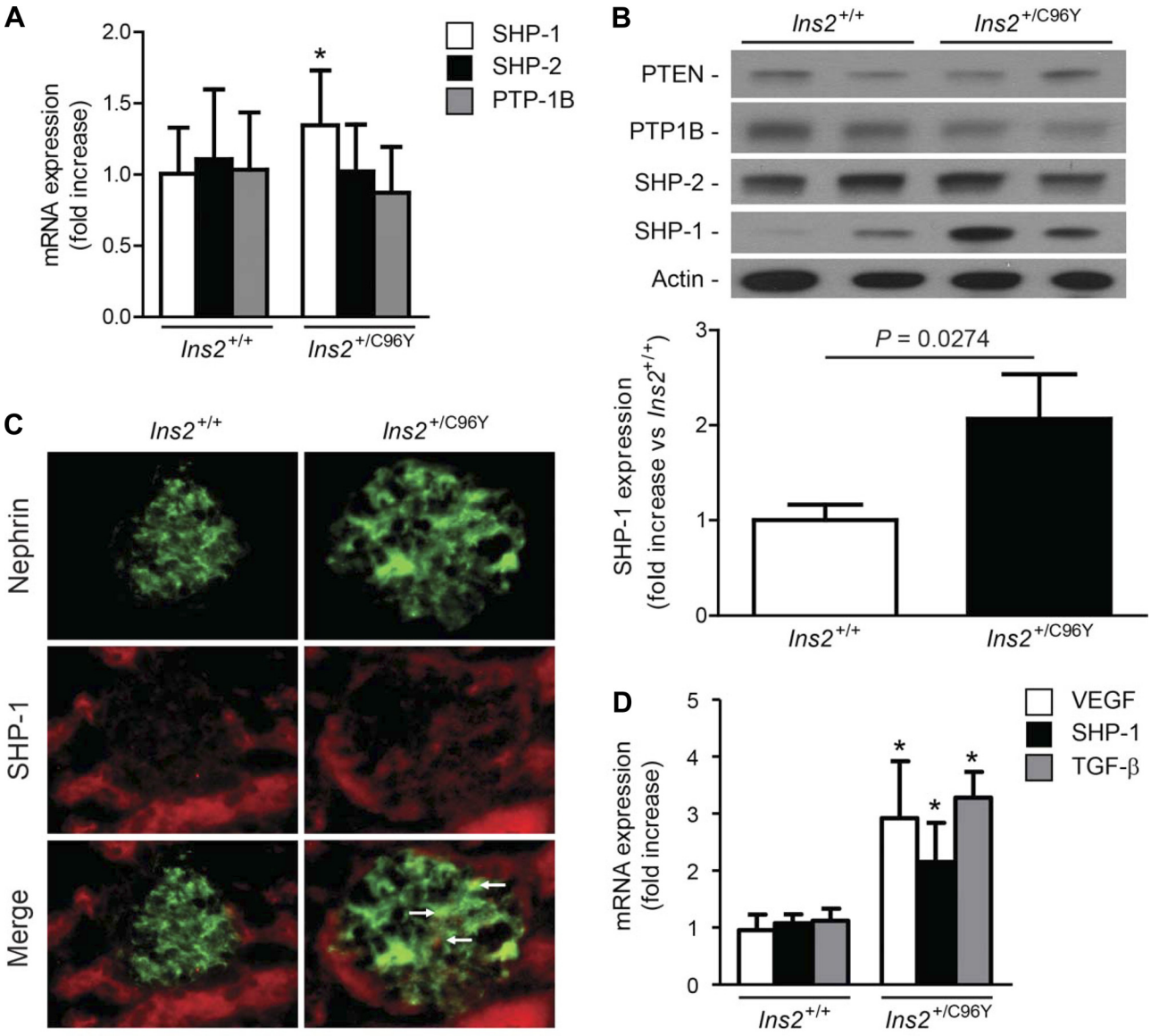

Fig. 5. Increased expression of Src homology-2 domain-containing phosphatase-1 (SHP-1) in renal glomeruli of *Ins2*$^{+/C96Y}$ mice. SHP-1, SHP-2, and protein tyrosine phosphatase (PTP) 1B mRNA (*A*) and protein (*B*) expression from renal cortex of *Ins2*$^{+/+}$ and *Ins2*$^{+/C96Y}$ mice. PTEN, phosphatase and tensin homolog. *C*: immunofluorescence labeling of podocytes (nephrin; green) and SHP-1 (red). *D*: vascular endothelial growth factor (VEGF), SHP-1, and TGF-β mRNA expression in glomeruli of *Ins2*$^{+/+}$ and *Ins2*$^{+/C96Y}$ mice. Protein expression was detected by Western blot, and densitometric quantitation was measured. Results are shown as means ± SD of 4–5 independent experiments. *$P < 0.05$ vs. *Ins2*$^{+/+}$ mice.

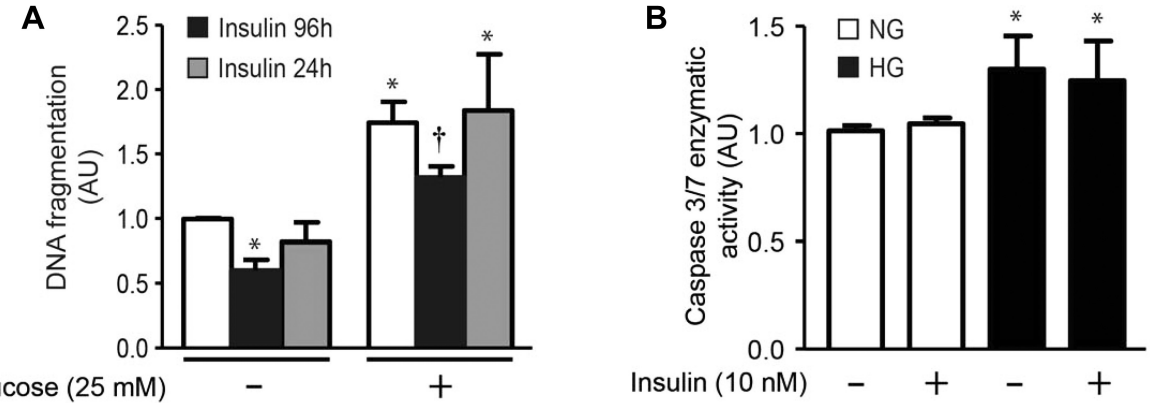

Fig. 6. High glucose levels induce podocyte apoptosis and caspase-3/7 activity. Podocytes were incubated with normal glucose (NG, 5.6 mM + 19.4 mM of mannitol) or high glucose (HG, 25 mM) for 96 h in the absence or presence of insulin for 96 h or during the last 24 h. DNA fragmentation (*A*) and caspase-3/7 (*B*) enzymatic activity were measured according to the manufacturer's instructions. $*P < 0.05$ vs. NG. $\dagger P < 0.05$ vs. NG + insulin (96 h).

last 24 h did not prevent HG effects on podocyte DNA fragmentation (Fig. 6*A*), suggesting that HG-induced insulin unresponsivess requires several hours of HG exposure. Caspase-3/7 enzymatic activity is also elevated in podocytes exposed to HG levels for 96 h and remained higher in the presence of insulin compared with the NG condition (Fig. 6*B*). These data suggest that hyperglycemia induced changes after several days and caused inhibition of insulin actions in podocytes. We then evaluated the insulin-signaling pathway in podocytes. In NG concentrations, insulin stimulation for 5 min enhanced the phosphorylation of IR-β, Akt, and ERK (Fig. 7). In contrast, podocytes exposed to elevated glucose levels showed a significant reduction of IR-β, Akt, and ERK phosphorylation.

Elevated glucose concentration-induced SHP-1 expression causes insulin inhibition. We have previously showed that high glucose levels increased SHP-1 expression in pericytes and podocytes (11, 22). We confirmed these results by showing that HG treatment enhanced SHP-1 mRNA and protein expression in podocytes by immunoblot, qPCR, and immunofluorescence analysis (Fig. 8, *A*, *B*, and *C*). In contrast, HG exposure did not change PTP1B, PTEN, or SHP-2 mRNA and protein expression in podocytes (Fig. 8, *A* and *B*). To link increased expression of SHP-1 and inhibition of insulin action, we examined its role using Ad-wtSHP-1 and Ad-dnSHP-1. Our data showed that overexpression of Ad-dnSHP-1 prevented HG-induced podocyte DNA fragmentation and caspase-3/7 enzymatic activity compared with control GFP-overexpressing podocytes (Fig. 9, *A* and *B*). In contrast, overexpressing SHP-1 wild type exacerbated HG-caused inhibition of insulin actions. We further examined the role of SHP-1 on the insulin-signaling pathway on Akt and ERK in podocytes. Overexpression of Ad-dnSHP-1 prevented HG effects by reestablishing insulin capacity to stimulate IR-β, Akt, and ERK compared with control GFP podocytes, whereas overexpression of wild-type SHP-1 completely blunted insulin stimulation on IR-β, Akt, and ERK phosphorylation exposed either to NG or HG (Fig. 9*C*). These data strongly support the notion that enhanced SHP-1 expression causes insulin inhibition and podocyte apoptosis.

SHP-1 interacts with IR-β to inhibit the insulin-signaling pathway. We investigated the mechanism of action by which SHP-1 reduces insulin action in podocytes exposed to HG levels. First, we performed qPCR analysis of IR-β, IRS-1, and IRS-2 in renal cortex and podocytes. Our data demonstrated that these genes were unaffected in the HG condition in podocytes and renal cortex of $Ins2^{+/C96Y}$ mice (data not shown). Coimmunoprecipitation assays indicated that SHP-1 association with IR-β is elevated in HG treatment but unchanged with IRS-1 in both podocytes exposed to HG levels ($P = 0.0464$) (Fig. 10*A*) and diabetic renal cortex of $Ins2^{+/C96Y}$ mice

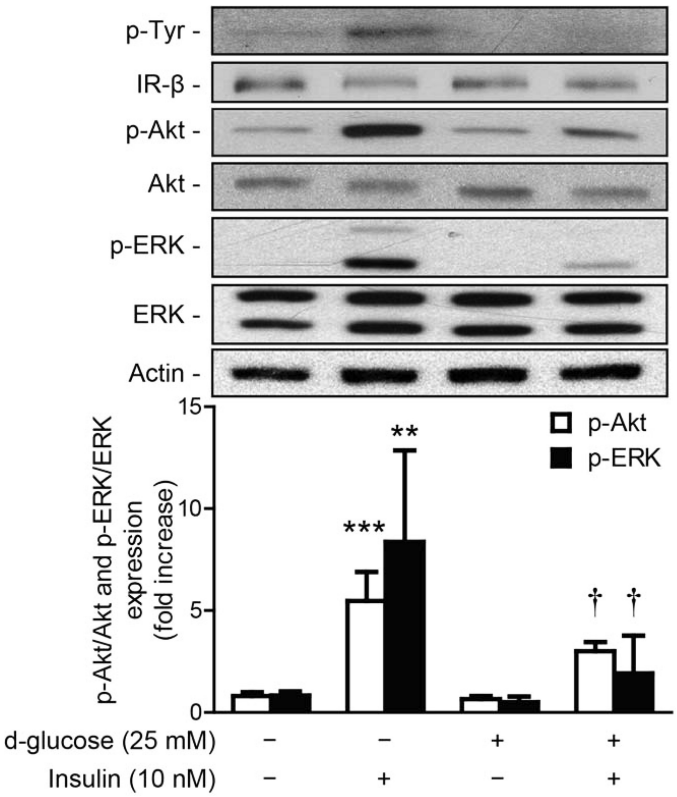

Fig. 7. Insulin signaling is blunted in podocytes exposed to high glucose levels. Podocytes were incubated with NG (5.6 mM + 19.4 mM of mannitol) or HG (25 mM) for 96 h followed by insulin stimulation for 5 min. Expression of phospho-tyrosine, IR-β, phospho-Akt, Akt, phospho-ERK, ERK, and actin was detected by Western blot, and densitometric quantitation was measured. Results are shown as means ± SD of 4–5 independent experiments. $**P < 0.01$ or $***P < 0.001$ vs. NG. $\dagger P < 0.05$ vs. NG + insulin.

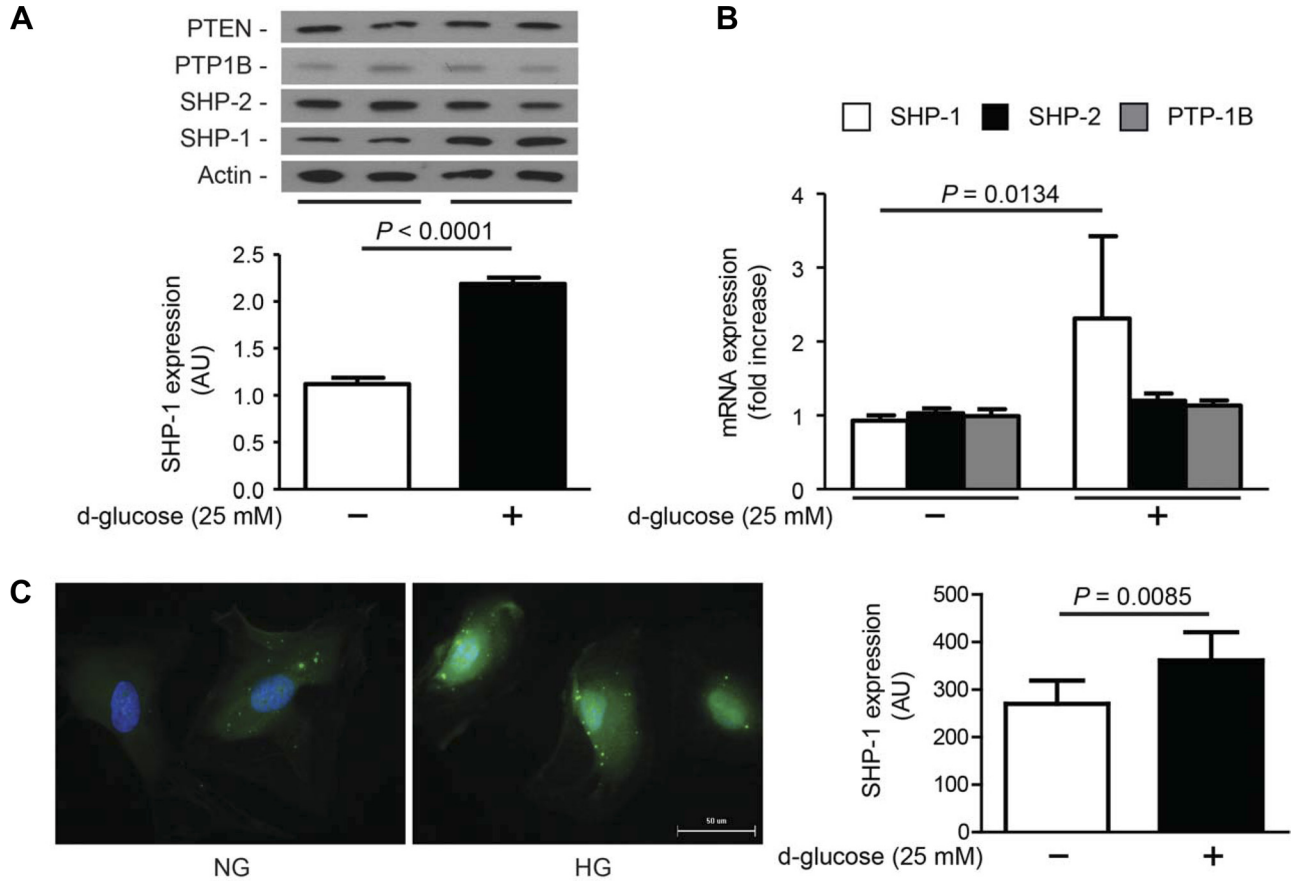

Fig. 8. Increased expression of SHP-1 in renal podocytes exposed to high glucose levels. Podocytes were incubated with NG (5.6 mM + 19.4 mM of mannitol) or HG (25 mM) for 96 h. *A*: protein expression of SHP-1, SHP-2, PTEN, and PTP1B was detected by Western blot, and densitometric quantitation was measured. *B*: SHP-1, SHP-2, and PTP1B mRNA expression. *C*: immunofluorescence of SHP-1 (green) from podocytes exposed to NG or HG. Results are shown as means ± SD of 3–5 independent experiments.

($P = 0.0077$) (Fig. 10*B*). Liver extract served as positive control for the coimmunoprecipitation assay. These data indicate that SHP-1 binds to IR-β to inhibit insulin actions.

DISCUSSION

Podocyte loss is an important determinant factor of DN and glomerulosclerosis, the leading cause of progression of kidney diseases. Superior to other markers of kidney injury, podocyte damage and depletion is probably the best early prognostic marker of nephropathy progression. Therefore, it is not surprising that an increasing number of basic and clinical studies have focused their attention to elucidate the mechanisms of podocyte loss in DN. More evidence suggests that insulin has multiple cellular functions on podocytes. In the present study, we hypothesized that hyperglycemia-induced SHP-1 expression in renal podocytes might have a significant role in podocyte function and survival. We demonstrated that SHP-1 binds with IR-β, preventing the insulin signaling pathway on Akt and ERK phosphorylation. Inhibition of SHP-1 restores insulin action and prevents podocyte apoptosis induced by HG levels.

Although the concept of insulin resistance has been largely attributed to type 2 diabetes, it is widely recognized that insulin resistance occurs in type 1 diabetes. This notion is supported by two clinical epidemiological studies that showed more cellular insulin resistance in type 1 patients with nephropathy compared with those without renal involvement (15, 26). Using a type 1 diabetic mouse model, we demonstrated that insulin-stimulated Akt and ERK phosphorylation is reduced in diabetic renal cortex compared with nondiabetic counterparts. The kidney has traditionally not been considered a target organ of insulin action. However, podocytes react similarly to insulin-stimulated glucose uptake kinetics and glucose transport (GLUT-1 and GLUT-4) expression as skeletal muscle and adipocytes (6). Furthermore, some evidence also suggested that rosiglitazone, a peroxisome proliferator-activated receptor-γ agonist, enhances GLUT-1 translocation in podocytes, increasing insulin sensitivity (20), and protects podocytes from injury (19). Although insulin has been shown to be essential for normal glomerular filtration, relatively little is known about cellular actions of insulin in podocytes. In an elegant study by Welsh and colleagues, podocyte-specific deletion of IR leads to the rapid development of albuminuria and glomerulosclerosis without diabetes (38). The loss of insulin-stimulated Akt phosphorylation has also been described in podocytes of the *db/db* model of type 2 diabetes (36, 51). The inability to signal through Akt is associated with increased susceptibility to podocyte death. In our study, we also observed that podocytes exposed to several days of high glucose levels inhibit insulin-stimulated Akt and ERK phosphorylation. Another study has extended our under-

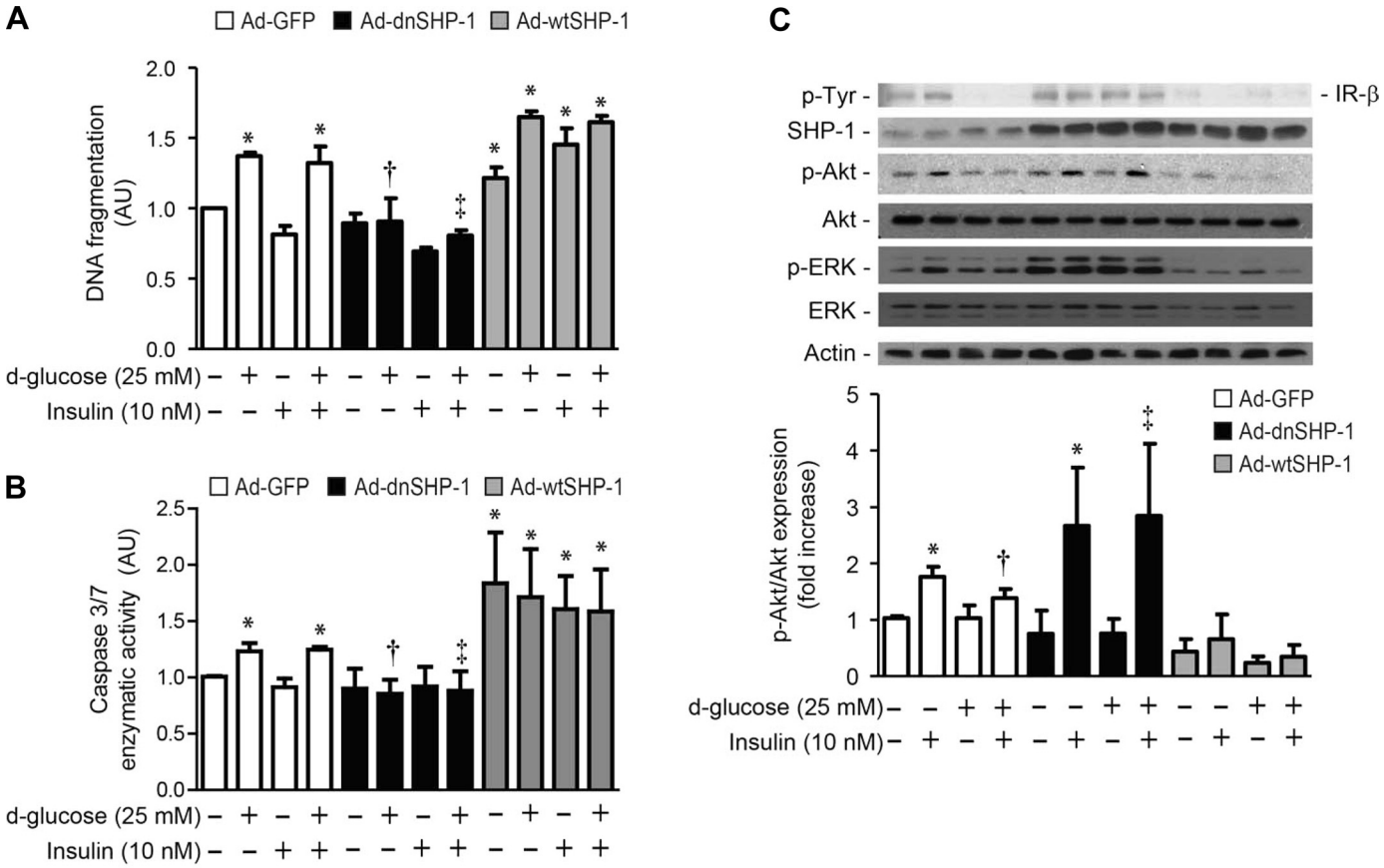

Fig. 9. Inhibition of SHP-1 prevents HG-induced podocyte apoptosis and restores insulin action. Podocytes were transfected with either adenoviral vectors containing green fluorescent protein (Ad-GFP, white bars), adenoviral vectors containing dominant-negative green fluorescent protein (Ad-dnSHP-1, black bars), or adenoviral vectors containing wild-type green fluorescent protein (Ad-wtSHP-1, gray bars) and then incubated with NG or HG for 96 h in the absence or presence of insulin. Apoptosis was measured by DNA fragmentation (*A*) and caspase-3/7 enzymatic activity (*B*) according to the manufacturer's instructions. *C*: expression of phospho-tyrosine of IR-β, phospho-Akt, Akt, phospho-ERK, ERK, SHP-1, and actin was detected by Western blot, and densitometric quantitation was measured. Results are shown as means ± SD of 3–4 independent experiments. *$P < 0.05$ vs. NG in Ad-GFP. †$P < 0.05$ vs. HG in Ad-GFP. ‡$P < 0.05$ vs. HG + insulin in Ad-GFP.

standing of the insulin signaling in the renal endothelial cells. With the use of two rat models of diabetes, experiments showed that diabetes decreases insulin capability to trigger IRS-1/Akt/eNOS phosphorylation in renal endothelial cells (23).

Reduction of podocyte density is a critical determinant for the development of proteinuria and the progression of kidney dysfunction in diabetic patients (34). Multiples studies using in vitro and in vivo mouse models of diabetes suggested that

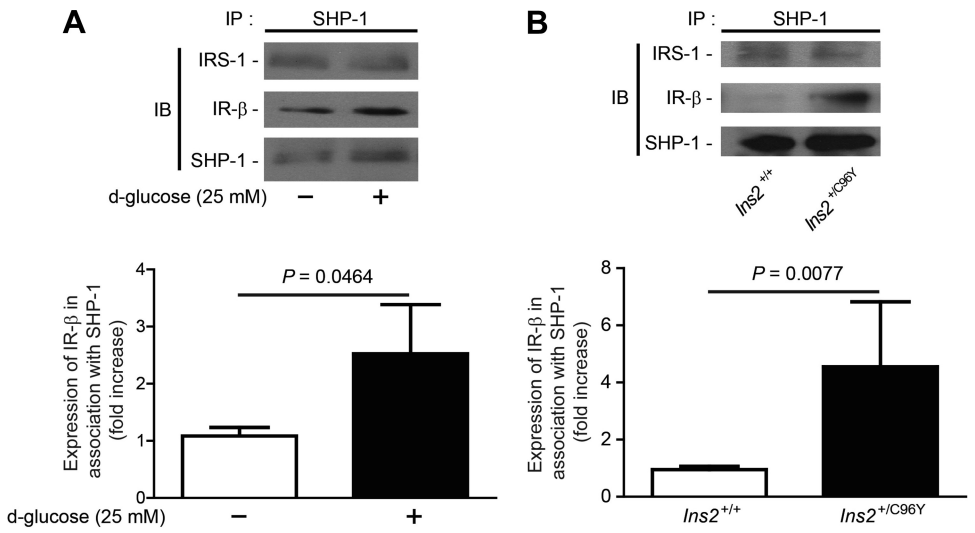

Fig. 10. SHP-1 interacts with IR-β. Podocytes were incubated with NG (5.6 mM + 19.4 mM of mannitol) or HG (25 mM) for 96 h. Coimmunoprecipitation of SHP-1 with either IR-β or IRS-1 in podocytes (*A*) and renal cortex (*B*) of $Ins2^{+/+}$ and $Ins2^{+/C96Y}$ mice. Protein expression was detected by Western blot, and densitometric quantitation was measured. IB, immunoblot. Results are shown as means ± SD of 3–4 independent experiments.

oxidative stress, activation of p38 mitogen-activated protein kinase, and TGF-β1 overexpression are involved in podocyte apoptosis (3, 31, 35). Besides insulin, several studies point to other growth factors such as the VEGF as essential for podocyte function and survival. VEGF expression is elevated in diabetic kidney (2, 16). Disruption of the *Vegfa* gene specifically in podocytes resulted in apoptosis of these cells, foot process effacement, loss of mesangial and endothelial cell fenestration, and death within the first days of life (8, 9). Evidence against an autocrine VEGF signaling loop in podocytes in vivo is in disagreement with previous data using cultured human and mouse podocytes (4, 10, 13). Interestingly, Sison et al. provide evidence that mouse podocytes in vivo express scant, if any, VEGFR2 and that podocyte-derived VEGFR2 does not contribute to the pathologies observed when there is too much or too little glomerular VEGF (33). This is in contrast with Mima and colleagues who have recently demonstrated that VEGFR2 signaling is altered in cultured podocytes exposed to high glucose levels (22).

The regulation of PTP, such as SHP-1, is an important mechanism for developmental control and homeostasis of an array of cellular processes, including cell growth, differentiation, mitotic cycle, and oncogenic transformation. SHP-1 knockout mice are markedly glucose tolerant and insulin sensitive compared with wild-type controls. Dubois and colleagues showed that these observations are due to the enhancement of the IR signaling by way of the IRS/phosphatidylinositol 3-kinase (PI3K)/Akt axis in the liver (7). Furthermore, SHP-1 regulates muscle insulin action in a cell-autonomous manner by negatively modulating both insulin signaling to Akt and GLUT-4 translocation, as well as GLUT-4 expression (1). In our current study, we showed that SHP-1 is associated with IR-β and interferes with insulin-induced Akt and ERK phosphorylation, which are blunted in podocytes exposed to high glucose levels. A previous study reported that the lipid phosphatase SHIP2 associates with CD2AP in podocyte, which can reduce insulin-stimulated Akt phosphorylation (17). However, this study was not performed under hyperglycemic conditions. Our study is the first to show that the increased expression of SHP-1 triggers insulin unresponsiveness in renal podocytes. Interestingly, with the use of an insulin-resistant type 2 diabetes model, previous data have reported that free fatty acids cause profound modifications in cultured podocytes, including decreased IR-β, IRS-1, and Akt expression (20). By contrast, our results did not show any significant changes in IRβ, IRS1, or IRS2 expression in podocytes or renal cortex of *Ins2*$^{+/C96Y}$ mice. Taken together, these data indicate that activation of SHP-1 and the consequent inhibition of insulin activity by SHP-1 contributed to the reduction of IR-β/IRS/PI3K/Akt phosphorylation. We cannot exclude the possibility that other mechanisms such as reactive oxygen species may be involved in HG-induced podocyte apoptosis independent of SHP-1. However, we believe that high glucose levels promote podocyte apoptosis through two important pathways: the increased oxidative stress/ROS production and the reduction of prosurvival factor action such as insulin and VEGF by triggering SHP-1 expression.

In conclusion, our study clearly demonstrated that insulin action is important in maintaining podocyte survival, and podocytes exposed to high glucose levels exhibit insulin resistance. The mechanisms causing insulin unresponsiveness by hyperglycemia are in part due to the increased association of SHP-1 with IR-β, which interferes with the insulin-stimulated Akt and ERK phosphorylation. Our study provides, for the first time, new insights into molecular mechanisms underlying hyperglycemia-induced insulin resistance in podocytes and will offer new attractive approaches to prevent kidney disease in patients with diabetes.

ACKNOWLEDGMENTS

The authors gratefully acknowledge Marie-Élaine Clavet (Montreal Heart Institute) for assistance with histochemistry technics.

GRANTS

This study was supported in part by grants from the Kidney Foundation of Canada, the Juvenile Diabetes Research Foundation, "Fonds de Recherche du Québec-Santé," and "Diabète Québec" to P. Geraldes and was performed at the Centre de Recherche Clinique Étienne-Le Bel, a research center funded by the "Fonds de Recherche du Québec-Santé". P. Geraldes is currently the recipient of a Scholarship Award from the Canadian Diabetes Association and the "Fonds de Recherche du Québec-Santé."

DISCLOSURES

No conflicts of interest, financial or otherwise, are declared by the authors.

AUTHOR CONTRIBUTIONS

Author contributions: N.D., F.L., B.D., A.G., and P.G. performed experiments; N.D., F.L., B.D., and P.G. analyzed data; N.D., F.L., B.D., C.R.K., and P.G. interpreted results of experiments; N.D., F.L., and P.G. prepared figures; N.D., C.R.K., and P.G. edited and revised manuscript; N.D. and P.G. approved final version of manuscript; P.G. conception and design of research; P.G. drafted manuscript.

REFERENCES

1. **Bergeron S, Dubois MJ, Bellmann K, Schwab M, Larochelle N, Nalbantoglu J, Marette A.** Inhibition of the protein tyrosine phosphatase SHP-1 increases glucose uptake in skeletal muscle cells by augmenting insulin receptor signaling and GLUT4 expression. *Endocrinology* 152: 4581–4588, 2011.
2. **Cha DR, Kim NH, Yoon JW, Jo SK, Cho WY, Kim HK, Won NH.** Role of vascular endothelial growth factor in diabetic nephropathy. *Kidney Int Suppl* 77: S104–S112, 2000.
3. **Chang JH, Paik SY, Mao L, Eisner W, Flannery PJ, Wang L, Tang Y, Mattocks N, Hadjadj S, Goujon JM, Ruiz P, Gurley SB, Spurney RF.** Diabetic kidney disease in FVB/NJ Akita mice: temporal pattern of kidney injury and urinary nephrin excretion. *PLoS One* 7: e33942, 2012.
4. **Chen S, Kasama Y, Lee JS, Jim B, Marin M, Ziyadeh FN.** Podocyte-derived vascular endothelial growth factor mediates the stimulation of alpha3(IV) collagen production by transforming growth factor-beta1 in mouse podocytes. *Diabetes* 53: 2939–2949, 2004.
5. **Collins AJ, Kasiske B, Herzog C, Chavers B, Foley R, Gilbertson D, Grimm R, Liu J, Louis T, Manning W, McBean M, Murray A, St Peter W, Xue J, Fan Q, Guo H, Li Q, Li S, Qiu Y, Li S, Roberts T, Skeans M, Snyder J, Solid C, Wang C, Weinhandl E, Zhang R, Arko C, Chen SC, Dalleska F, Daniels F, Dunning S, Ebben J, Frazier E, Hanzlik C, Johnson R, Sheets D, Wang X, Forrest B, Berrini D, Constantini E, Everson S, Eggers P, Agodoa L.** Excerpts from the United States Renal Data System 2006 Annual Data Report. *Am J Kidney Dis* 49: S1–S296, 2007.
6. **Coward RJ, Welsh GI, Yang J, Tasman C, Lennon R, Koziell A, Satchell S, Holman GD, Kerjaschki D, Tavare JM, Mathieson PW, Saleem MA.** The human glomerular podocyte is a novel target for insulin action. *Diabetes* 54: 3095–3102, 2005.
7. **Dubois MJ, Bergeron S, Kim HJ, Dombrowski L, Perreault M, Fournes B, Faure R, Olivier M, Beauchemin N, Shulman GI, Siminovitch KA, Kim JK, Marette A.** The SHP-1 protein tyrosine phosphatase negatively modulates glucose homeostasis. *Nat Med* 12: 549–556, 2006.
8. **Eremina V, Cui S, Gerber H, Ferrara N, Haigh J, Nagy A, Ema M, Rossant J, Jothy S, Miner JH, Quaggin SE.** Vascular endothelial growth factor a signaling in the podocyte-endothelial compartment is required for

mesangial cell migration and survival. *J Am Soc Nephrol* 17: 724–735, 2006.
9. **Eremina V, Sood M, Haigh J, Nagy A, Lajoie G, Ferrara N, Gerber HP, Kikkawa Y, Miner JH, Quaggin SE.** Glomerular-specific alterations of VEGF-A expression lead to distinct congenital and acquired renal diseases. *J Clin Invest* 111: 707–716, 2003.
10. **Foster RR, Hole R, Anderson K, Satchell SC, Coward RJ, Mathieson PW, Gillatt DA, Saleem MA, Bates DO, Harper SJ.** Functional evidence that vascular endothelial growth factor may act as an autocrine factor on human podocytes. *Am J Physiol Renal Physiol* 284: F1263–F1273, 2003.
11. **Geraldes P, Hiraoka-Yamamoto J, Matsumoto M, Clermont A, Leitges M, Marette A, Aiello LP, Kern TS, King GL.** Activation of PKC-delta and SHP-1 by hyperglycemia causes vascular cell apoptosis and diabetic retinopathy. *Nat Med* 15: 1298–1306, 2009.
12. **Greenbaum CJ.** Insulin resistance in type 1 diabetes. *Diabetes Metab Res Rev* 18: 192–200, 2002.
13. **Guan F, Villegas G, Teichman J, Mundel P, Tufro A.** Autocrine VEGF-A system in podocytes regulates podocin and its interaction with CD2AP. *Am J Physiol Renal Physiol* 291: F422–F428, 2006.
14. **Gurley SB, Mach CL, Stegbauer J, Yang J, Snow KP, Hu A, Meyer TW, Coffman TM.** Influence of genetic background on albuminuria and kidney injury in Ins2(+/C96Y) (Akita) mice. *Am J Physiol Renal Physiol* 298: F788–F795, 2010.
15. **Hadjadj S, Pean F, Gallois Y, Passa P, Aubert R, Weekers L, Rigalleau V, Bauduceau B, Bekherraz A, Roussel R, Dussol B, Rodier M, Marechaud R, Lefebvre PJ, Marre M.** Different patterns of insulin resistance in relatives of type 1 diabetic patients with retinopathy or nephropathy: the Genesis France-Belgium Study. *Diabetes Care* 27: 2661–2668, 2004.
16. **Hovind P, Tarnow L, Oestergaard PB, Parving HH.** Elevated vascular endothelial growth factor in type 1 diabetic patients with diabetic nephropathy. *Kidney Int Suppl* 75: S56–S61, 2000.
17. **Hyvonen ME, Saurus P, Wasik A, Heikkila E, Havana M, Trokovic R, Saleem M, Holthofer H, Lehtonen S.** Lipid phosphatase SHIP2 downregulates insulin signalling in podocytes. *Mol Cell Endocrinol* 328: 70–79, 2010.
18. **Jauregui A, Mintz DH, Mundel P, Fornoni A.** Role of altered insulin signaling pathways in the pathogenesis of podocyte malfunction and microalbuminuria. *Curr Opin Nephrol Hypertens* 18: 539–545, 2009.
19. **Kanjanabuch T, Ma LJ, Chen J, Pozzi A, Guan Y, Mundel P, Fogo AB.** PPAR-gamma agonist protects podocytes from injury. *Kidney Int* 71: 1232–1239, 2007.
20. **Lennon R, Welsh GI, Singh A, Satchell SC, Coward RJ, Tavare JM, Mathieson PW, Saleem MA.** Rosiglitazone enhances glucose uptake in glomerular podocytes using the glucose transporter GLUT1. *Diabetologia* 52: 1944–1952, 2009.
21. **Meyer TW, Bennett PH, Nelson RG.** Podocyte number predicts long-term urinary albumin excretion in Pima Indians with Type II diabetes and microalbuminuria. *Diabetologia* 42: 1341–1344, 1999.
22. **Mima A, Kitada M, Geraldes P, Li Q, Matsumoto M, Mizutani K, Qi W, Li C, Leitges M, Rask-Madsen C, King GL.** Glomerular VEGF resistance induced by PKCdelta/SHP-1 activation and contribution to diabetic nephropathy. *FASEB J* 2012.
23. **Mima A, Ohshiro Y, Kitada M, Matsumoto M, Geraldes P, Li C, Li Q, White GS, Cahill C, Rask-Madsen C, King GL.** Glomerular-specific protein kinase C-beta-induced insulin receptor substrate-1 dysfunction and insulin resistance in rat models of diabetes and obesity. *Kidney Int* 79: 883–896, 2011.
24. **Mundel P, Reiser J, Zuniga Mejia Borja A, Pavenstadt H, Davidson GR, Kriz W, Zeller R.** Rearrangements of the cytoskeleton and cell contacts induce process formation during differentiation of conditionally immortalized mouse podocyte cell lines. *Exp Cell Res* 236: 248–258, 1997.
25. **Musso C, Javor E, Cochran E, Balow JE, Gorden P.** Spectrum of renal diseases associated with extreme forms of insulin resistance. *Clin J Am Soc Nephrol* 1: 616–622, 2006.
26. **Orchard TJ, Chang YF, Ferrell RE, Petro N, Ellis DE.** Nephropathy in type 1 diabetes: a manifestation of insulin resistance and multiple genetic susceptibilities? Further evidence from the Pittsburgh Epidemiology of Diabetes Complication Study. *Kidney Int* 62: 963–970, 2002.
27. **Oudit GY, Liu GC, Zhong J, Basu R, Chow FL, Zhou J, Loibner H, Janzek E, Schuster M, Penninger JM, Herzenberg AM, Kassiri Z, Scholey JW.** Human recombinant ACE2 reduces the progression of diabetic nephropathy. *Diabetes* 59: 529–538, 2010.
28. **Pagtalunan ME, Miller PL, Jumping-Eagle S, Nelson RG, Myers BD, Rennke HG, Coplon NS, Sun L, Meyer TW.** Podocyte loss and progressive glomerular injury in type II diabetes. *J Clin Invest* 99: 342–348, 1997.
29. **Qi Z, Whitt I, Mehta A, Jin J, Zhao M, Harris RC, Fogo AB, Breyer MD.** Serial determination of glomerular filtration rate in conscious mice using FITC-inulin clearance. *Am J Physiol Renal Physiol* 286: F590–F596, 2004.
30. **Sarnak MJ, Levey AS, Schoolwerth AC, Coresh J, Culleton B, Hamm LL, McCullough PA, Kasiske BL, Kelepouris E, Klag MJ, Parfrey P, Pfeffer M, Raij L, Spinosa DJ, Wilson PW.** Kidney disease as a risk factor for development of cardiovascular disease: a statement from the American Heart Association Councils on Kidney in Cardiovascular Disease, High Blood Pressure Research, Clinical Cardiology, and Epidemiology and Prevention. *Circulation* 108: 2154–2169, 2003.
31. **Schiffer M, Bitzer M, Roberts IS, Kopp JB, ten Dijke P, Mundel P, Bottinger EP.** Apoptosis in podocytes induced by TGF-beta and Smad7. *J Clin Invest* 108: 807–816, 2001.
32. **Shankland SJ, Pippin JW, Reiser J, Mundel P.** Podocytes in culture: past, present, and future. *Kidney Int* 72: 26–36, 2007.
33. **Sison K, Eremina V, Baelde H, Min W, Hirashima M, Fantus IG, Quaggin SE.** Glomerular structure and function require paracrine, not autocrine, VEGF-VEGFR-2 signaling. *J Am Soc Nephrol* 21: 1691–1701, 2010.
34. **Steffes MW, Schmidt D, McCrery R, Basgen JM.** Glomerular cell number in normal subjects and in type 1 diabetic patients. *Kidney Int* 59: 2104–2113, 2001.
35. **Susztak K, Raff AC, Schiffer M, Bottinger EP.** Glucose-induced reactive oxygen species cause apoptosis of podocytes and podocyte depletion at the onset of diabetic nephropathy. *Diabetes* 55: 225–233, 2006.
36. **Tejada T, Catanuto P, Ijaz A, Santos JV, Xia X, Sanchez P, Sanabria N, Lenz O, Elliot SJ, Fornoni A.** Failure to phosphorylate AKT in podocytes from mice with early diabetic nephropathy promotes cell death. *Kidney Int* 73: 1385–1393, 2008.
37. **Tryggvason K, Patrakka J, Wartiovaara J.** Hereditary proteinuria syndromes and mechanisms of proteinuria. *N Engl J Med* 354: 1387–1401, 2006.
38. **Welsh GI, Hale LJ, Eremina V, Jeansson M, Maezawa Y, Lennon R, Pons DA, Owen RJ, Satchell SC, Miles MJ, Caunt CJ, McArdle CA, Pavenstadt H, Tavare JM, Herzenberg AM, Kahn CR, Mathieson PW, Quaggin SE, Saleem MA, Coward RJ.** Insulin signaling to the glomerular podocyte is critical for normal kidney function. *Cell Metab* 12: 329–340, 2010.
39. **White KE, Bilous RW, Marshall SM, El Nahas M, Remuzzi G, Piras G, De Cosmo S, Viberti G.** Podocyte number in normotensive type 1 diabetic patients with albuminuria. *Diabetes* 51: 3083–3089, 2002.
40. **Yip J, Mattock MB, Morocutti A, Sethi M, Trevisan R, Viberti G.** Insulin resistance in insulin-dependent diabetic patients with microalbuminuria. *Lancet* 342: 883–887, 1993.